 doi:10.20944/preprints202208.0341.v1

Article

An Integrative Analysis Identified Schizophrenia-Associated Brain Cell Types and Gene Expression Changes

Wenxiang Cai[1], Weichen Song[1], Zhe Liu[1], Dhruba Tara Maharjan[1], Jisheng Liang[1], Guan Ning Lin[1,2,*]

[1] Shanghai Mental Health Center, Shanghai Jiao Tong University School of Medicine, School of Biomedical Engineering, Shanghai Jiao Tong University, Shanghai, China; caiwenxiang@sjtu.edu.cn (W.C.); goubegou@sjtu.edu.cn (W.S.); liuzlm1030@sjtu.edu.cn (Z.L.); x387735517@sjtu.edu.cn (D.T.M.); kense_leung@sjtu.edu.cn (J.L.)

[2] Shanghai Key Laboratory of Psychotic Disorders, Shanghai, China

* Correspondence: nickgnlin@sjtu.edu.cn

Abstract: Schizophrenia (SCZ) is a severe mental disorder that may result in hallucinations, delusions, and extremely disordered thinking. How each cell type in the brain contributes to SCZ occurrence is still unclear. Here, we leveraged the human dorsolateral prefrontal cortex bulk RNA-seq data, then used the RNA-seq deconvolution algorithm CIBERSORTx to generate SCZ brain single-cell RNA-seq data for a comprehensive analysis to understand SCZ-associated brain cell types and gene expression changes. Firstly, we observed that the proportions of brain cell types in SCZ differed from normal samples. Among these cell types, astrocyte, pericyte, and PAX6 cells were found to have a higher proportion in SCZ patients (astrocyte: SCZ = 0.163, Control = 0.145, P.adj = 4.9×10-4; pericyte: SCZ = 0.057, Control = 0.066, P.adj = 1.1×10-4; PAX6 : SCZ = 0.014, Control = 0.011, P.adj = 0.014), while the L5/6_IT_CAR3 cells and LAMP5 cells are the exact opposite (L5/6_IT_Car3 : SCZ = 0.102, Control = 0.108, P.adj = 0.016; LAMP5 : SCZ = 0.057, Control = 0.066, P.adj = 2.2×10-6). Next, we investigated gene expression in cell types and functional pathways in SCZ. We observed chemical synaptic transmission dysregulation in two types of GABAergic neurons (PVALB and LAMP5), and immune reaction involvement in GABAergic neurons (SST) and non-neuronal cell types (endothelial and oligodendrocyte). Furthermore, we observed that some differential expression genes from bulk RNA-seq displayed cell-type-specific abnormal in the expression of molecules in SCZ. Finally, the cell types with the SCZ-related transcriptomic changes could be considered to belong to the same module since we observed two major similar coordinated transcriptomic changes across these cell types. Together, our results offer novel insights into cellular heterogeneity and the molecular mechanisms underlying SCZ.

Keywords: Schizophrenia; cell types proportions; differential expression genes; functional pathways; CIBERSORTx

1. Introduction

Schizophrenia (SCZ) is a neuropsychiatric disorder characterized by disorganized speech, auditory hallucinations, and cognitive impairment [1]. SCZ affects approximately 1% of the worldwide population [2]. Most SCZ patients are affected by genetic and early environmental risk factors that disrupt brain development, particularly in some neuronal subtypes and brain regions [3].

Many efforts have already been carried out to investigate the pathology of the disease. Some studies show that the dorsolateral prefrontal cortex (DLPFC) is a crucial region associated with cognitive deficits and working memory [4, 5]. Abnormal bioenergetic pathways have been reported in schizophrenia in DLPFC, including a decrease in the expression of genes encoding proteins involving the malate shuttle, tricarboxylic acid (TCA) cycle, and ubiquitin metabolism [6]. Moreover, impaired neuronal signaling in the DLPFC can influence synchronized patterns of neural activity that ultimately influence cognition and behavior [7]. However, brain cell types have not been thoroughly studied in SCZ, and

 doi:10.20944/preprints202208.0341.v1

not all brain cell types would be similarly affected in SCZ. It is essential to identify the contribution of each cell type to SCZ. For instance, GABAergic neurons provide both inhibitory and disinhibitory modulation of cortical and hippocampal circuits, and it was reported that these functions are altered in schizophrenic (SCZ) subjects [8-10]. Astrocytes can critically affect key neurodevelopmental and homeostatic processes of schizophrenia pathogenesis, including glutamatergic signaling, synaptogenesis, synaptic pruning, and myelination [11, 12]. In addition, a common-variant genome-wide association results for SCZ from mouse map to a limited set of brain cells such as pyramidal cells, medium spiny neurons (MSNs), and certain interneurons, but far less consistently to an embryonic, progenitor, or glial cells [13].

Meanwhile, using multi-omics integrative analysis to explore the pathogenesis of SCZ has already resulted in hundreds of genetic loci being identified to associate with SCZ [14]. Although such studies provided some information about SCZ-related cell types and potential critical genes, they focused only on a certain type of brain or used omics data from mouse models instead of human patients. These results are not comprehensive enough to confirm and decipher the genetic and molecular mechanisms of SCZ. Thus, it is important to apply single-cell RNA sequencing (scRNA-seq) on human SCZ samples, which allows us to explore the cell composition and cell-type-specific molecular alterations at the single-cell level.

Limited by the lack of single-cell RNA-seq data from human SCZ patients, we used CIBERSORTx [15], a tool that can estimate cell type abundances from bulk tissue transcriptomes and infers cell-type-specific gene expression profiles and allows the use of single-cell RNA-sequencing data without single-cell sorting.

In this study, we provided large-scale changes in the neuronal and non-neuronal transcriptomes of SCZ patients using CIBERSORTx. Especially, we showed that some cell types exhibited cell proportion changes and a dramatic SCZ-related cell-special dysregulation of gene expression. Next, by performing gene ontology analysis on these DEGs of each cell type, we observed cell-type-special function pathways underlying SCZ. Moreover, we identified ten genes that overlapped between bulk RNA-seq and scRNA-seq DEGs and their cell-type-special changes pattern. In addition, we estimated the Jaccard similarity score among each cell type to identify which cell types belong to the same module. Thus, our results indicate that the SCZ-related cell types and cell-type-special gene expression changes could help understand and study the potential pathogenic mechanism in SCZ.

2. Results

2.1. Identification of changes of cell-type proportion using Signature Matrix

We downloaded 6,468 cell samples single-cell RNA-seq data [16, 17] clustered from 19 neuronal and non-neuronal cell types (L4_ IT, L5_ET, L5/6_NP, L5/6_IT_CAR3, L6_CT, L6b, IT, LAMP5, SST, VIP, Astrocyte, Endothelial, Microglia, Oligodendrocyte, OPC, Pericyte, and VLMC) isolated from MTG and ACC tissues from normal adults. Based on the CIBERSORTx algorithm, a signature matrix including genes of 19 cell types was created (Figure 1a). We also downloaded RNA-seq data of schizophrenia patients and normal controls from BrainSeq Phase 2 [18].

Next, to identify the proportion change of each cell type of bulk samples, applying the CIBERSORTx algorithm to RNA-seq data with the signature matrix obtained above, we estimated the relative proportions of 19 neuron and non-neuron cell subsets of DLPFC between SCZ patients and normal samples (Figure 1b). Within all brain cell types, astrocyte, pericyte, and PAX6 cells were found to have a higher proportion in SCZ patients than in normal people (astrocyte: SCZ = 0.163, Control = 0.145, P.adj = 4.9×10^{-4}; pericyte: SCZ = 0.057, Control = 0.066, P.adj = 1.1×10^{-4}; PAX6: SCZ = 0.014, Control = 0.011, P.adj = 0.014). In addition, we observed a notable decrease in the proportion of several cell types, such as the L5/6_IT_CAR3 cell type and LAMP5 cell type (L5/6_IT_Car3: SCZ = 0.102,

 doi:10.20944/preprints202208.0341.v1

Control = 0.108, P.adj = 0.016; LAMP5: SCZ = 0.057, Control = 0.066, P.adj = 2.2×10^{-6}). The rest of the cell types had no significant differences between SCZ patients and normal controls.

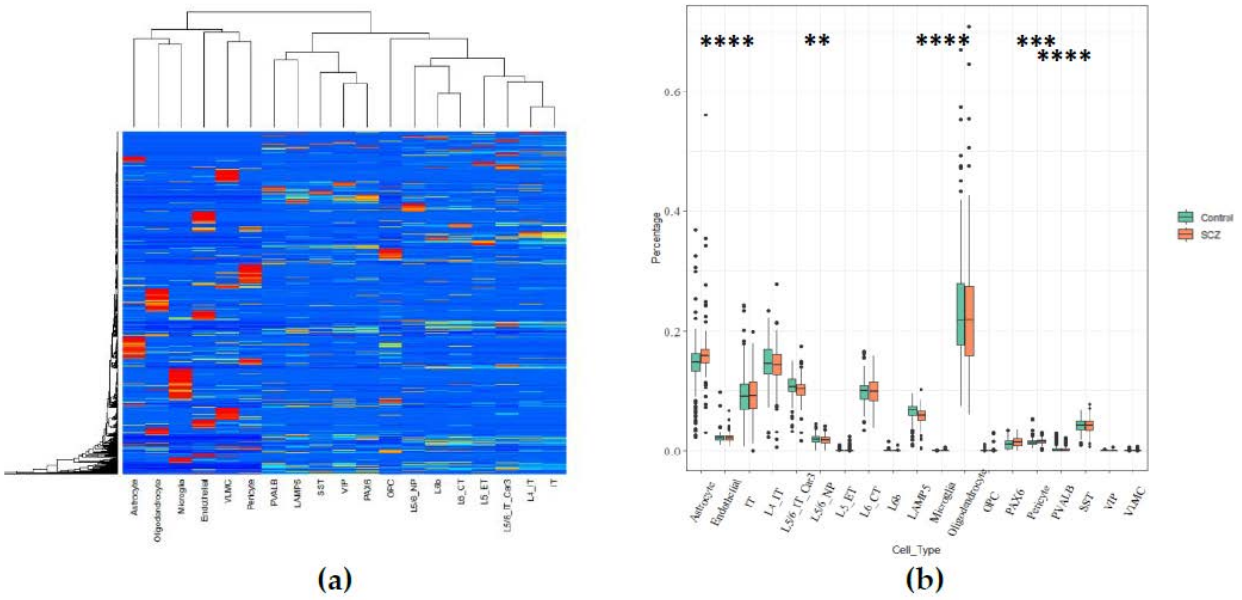

Figure 1. Distribution of brain cell types in bulk RNA-seq data. (**a**) Signature gene matrix of inferred 19 brain cell types by study. Heatmap showing a custom signature matrix created from scRNA-seq data with CIBERSORTx; (**b**) box plots depict distributions of 19 brain neuronal and non-neuronal cell types between SCZ and normal samples (depicted p-values are from the Wilcoxon test). *p < 0.05; **p < 0.01; ***p < 0.001; ****p < 0.0001.

2.2. Bulk RNA-seq revealed abnormal gene expression and immune related pathways in SCZ samples

To identify gene expression change and whether these DEGs enriched functional pathways associated with SCZ, we first used the bulk RNA-seq data for differential analysis. Taking the overlapped results from differential expression genes (DEGs) from three R packages "DESeq-2 [20]", "limma [21]", "edgeR [22]", 108 DEGs (77 down-regulated and 31 up-regulated) were detected. (Figure 2a). Next, we applied gene enrichment (GO) analysis to the DEGs. We observed that the enrichment of DEGs was associated with gene ontology biological processes (BP) terms related to neutrophil degranulation, neutrophil activation involved in immune response, regulation of inflammatory response, and so on (Figure 2b). In addition, the enrichment of DEGs was associated with gene ontology Molecular Function (MF) terms related to functions, such as cytokine receptor activity, immune receptor activity, NAD^+ nucleosidase activity (Figure 2c). The analysis showed that DEGs of bulk RNA-seq converged to immune-related pathways, further indicating that immune response played a significant role in SCZ pathogenesis.

Preprints (www.preprints.org) | NOT PEER-REVIEWED | Posted: 18 August 2022 doi:10.20944/preprints202208.0341.v1

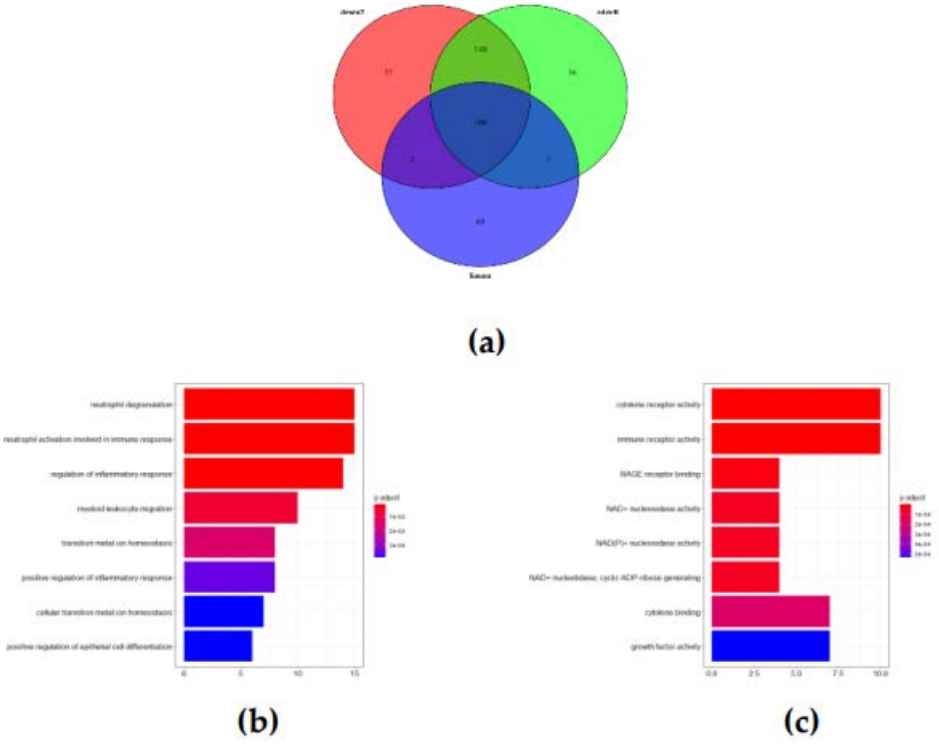

Figure 2. DEGs and related pathways of bulk RNA-seq. (**a**) Venn diagram of DEGs by three differential expression algorithms (DEseq2, LIMMA, and edgeR); (**b, c**) The top significantly overrepresented GO BP and MF terms. The x-axis represents the count of genes. The y-axis indicates the items of GO BP. The color represents the value of the FDR adjusted p-value

2.3. PVALB+, SST+ and LAMP5+ neurons involved in chemical synaptic transmission and immune function dysregulation in SCZ

Next, we investigate the patterns of expression difference of DEGs in each cell types in SCZ. Based on the gene expression profiles of each cell type from CRBERSORTX group-mode analysis, we compared gene expression profiles from SCZ and control samples for each cell type following CIBERSORTx guidelines [24]. At the threshold of false discovery rate (FDR) of < 0.05 and |log2 fold change| > 1.6 (PVALB cell type |log2 fold change| > 1.6), we identified the DEGs for each neuronal cell type (Figure.3a; Table S1). PVALB$^+$, SST$^+$ and LAMP5$^+$ neurons had the largest number of DEGs. We conducted a functional enrichment analysis on DEGs of each cell type, respectively (Figure.3b), to identify SCZ-associated pathways shared across neuronal cell types and those specific to individual cell types. First, we observed that PVALB$^+$ neuron was significantly enriched with gene ontology terms related to modulation of chemical synaptic transmission, synaptic signaling, postsynapse, and dendrite (Figure.3b). We than found that LAMP5$^+$ neuron was significantly enriched with gene ontology terms related to axodendritic transport, chemical synaptic transmission, axon development, anion transmembrane transport, axon, postsynapse (Figure.3c). Moreover, functional enrichment analysis indicated that the terms chemical synaptic transmission and postsynapse were enriched in DEGs in both PVALB$^+$ and LAMP5$^+$ neuron. This result suggested that both cell types were involved in chemical synaptic transmission dysregulation in schizophrenia. SST cell type was significantly enriched with gene ontology terms related to positive regulation of neutrophil degranula-

Preprints (www.preprints.org) | NOT PEER-REVIEWED | Posted: 18 August 2022 doi:10.20944/preprints202208.0341.v1

tion and positive regulation of leukocyte cell-cell adhesion (Figure.3d). This result suggested that SST cell type was associated with immune function dysregulation in schizophrenia. No significance was observed for any of the other cell types.

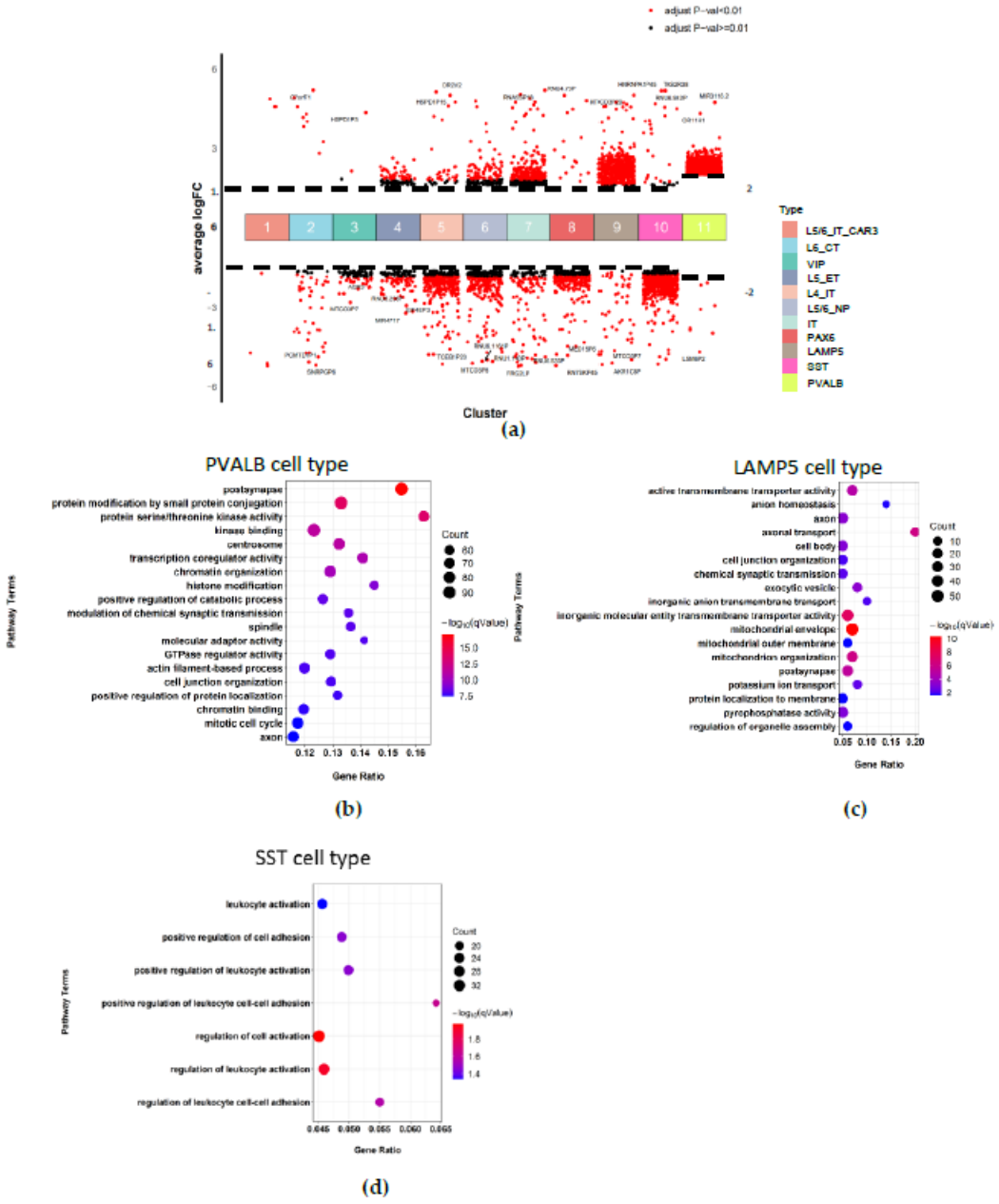

Figure 3. neuronal type-special DEGs and related pathways of scRNA-seq. (**a**) Differential gene expression analysis showing up- and down-regulated genes across all 11 neuronal clusters. An adjusted p-value < 0.01 is indicated in red, while an adjusted p-value ≥ 0.01 is indicated in black; (**b-d**) The top significantly overrepresented GO terms. The x-axis represents the gene ratio. The y-axis indicates the items of GO, the color of dots represents the value of -log (FDR adjusted p-value), and the size of dots represents the count of genes.

2.4. Oligodendrocyte and endothelial involved in immune function dysregulation in SCZ

Next, we analyzed the SCZ-associated pathways of each non-neuronal cell type. Under the threshold of false discovery rate (FDR) of < 0.05 and |log2 fold change| > 1.5, we identified the DEGs for each non-neuronal cell type and visualized them by volcano plots (Figure.4a; Table S2). Oligodendrocytes and Endothelial exhibited the top 2 number of DEGs. To identify SCZ-associated pathways that were shared across non-neuronal cell

Preprints (www.preprints.org) | NOT PEER-REVIEWED | Posted: 18 August 2022 doi:10.20944/preprints202208.0341.v1

types and those that were specific for individual cell types, we conducted a functional enrichment analysis on DEGs of each cell type, respectively. Oligodendrocyte was significantly enriched with gene ontology terms related to defense response to a virus, pattern recognition receptor signaling pathway, and inflammatory response (Figure.4b). Endothelial was significantly enriched with gene ontology terms related to chemokine receptor binding (Figure.4c). This result suggested that both oligodendrocyte and endothelial were associated with immune function dysregulation in schizophrenia. No significant enrichment was observed for any of the other cell types.

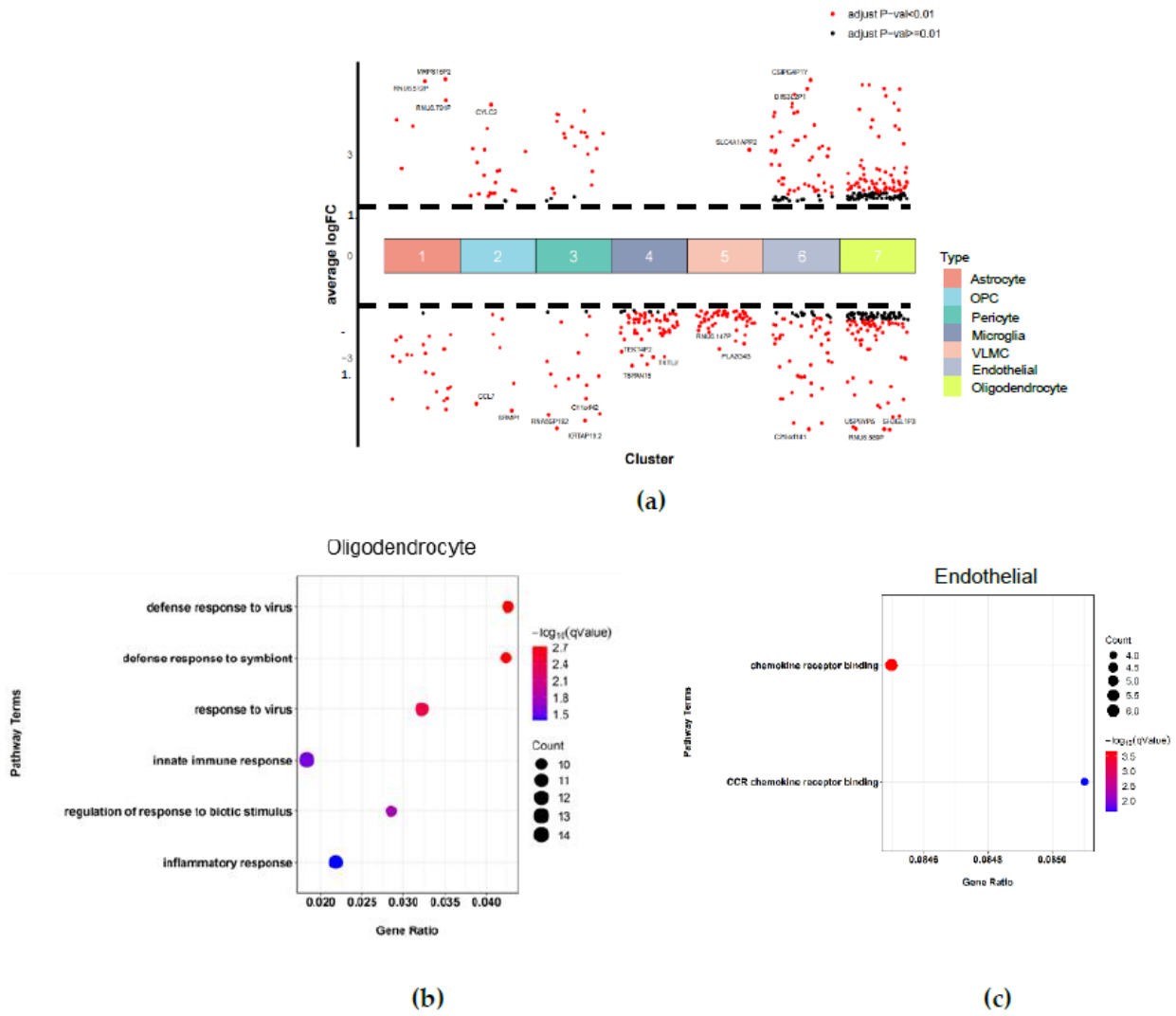

Figure 4. non-neuronal type-special DEGs and related pathways of scRNA-seq. (**a**) Differential gene expression analysis showing up- and down-regulated genes across all 7 non-neuronal clusters. An adjusted p value < 0.01 is indicated in red, while an adjusted p value ≥ 0.01 is indicated in black; (**b, c**) The top significantly GO terms. The x-axis represents the gene ratio, the y-axis indicates the items of GO, the color of dots represents the value of -log (FDR adjusted p-value), the size of dots represents the count of genes.

2.5. Bulk RNA-seq DEGs expression changes at the cellular layer

To explore specific changes in the expression of molecules in each cell type in the brain DLPFC region, we evaluated the changes in the expression of bulk RNA-seq DEGs in the cell layer. There are ten genes (TNFRSF13C, MPEG1, OSMR, KDF1, GDNF, TDGF1, C4B, SERPINA5, DPPA2P4, and IL18RAP) overlapped between bulk RNA-seq and

Preprints (www.preprints.org) | NOT PEER-REVIEWED | Posted: 18 August 2022 doi:10.20944/preprints202208.0341.v1

scRNA-seq DEGs (figure 5a). Then, we attempted to explore the cellular level expression changes of these genes. After filtration of low-quality genes, we finally gained expression changes of 10 DEGs in 5 cell types. As shown in figure 5b, most of the DEGs exhibited expression significantly dysregulated in SST and PVALB cell types. For SST cell type, TNFRSFQ13C and MPEG1, which were related to immune response [25-26], were significantly downregulated. TDGF1, known for playing a crucial role in human brain development [27], was also downregulated in SST cell types. For PVALB cell type, SERPINA5, which is implicated in synaptic plasticity and memory formation [28] and was downregulated in bulk RNA-seq, was also downregulated in IT, PVALB cell types. IL18RAP, known as a proinflammatory cytokine involved in inducing cell-mediated immunity [29], was upregulated in PVALB cell types. In addition, GDNF, which has been reported that the endogenous dosage correlates with clinical severity in schizophrenia [30], was upregulated in oligodendrocytes. C4B, which is involved in synaptic phagocytosis [31], was downregulated in L4_IT cell type. Taken together, we found that the expression changes of several SCZ-related genes are cell-type-specific.

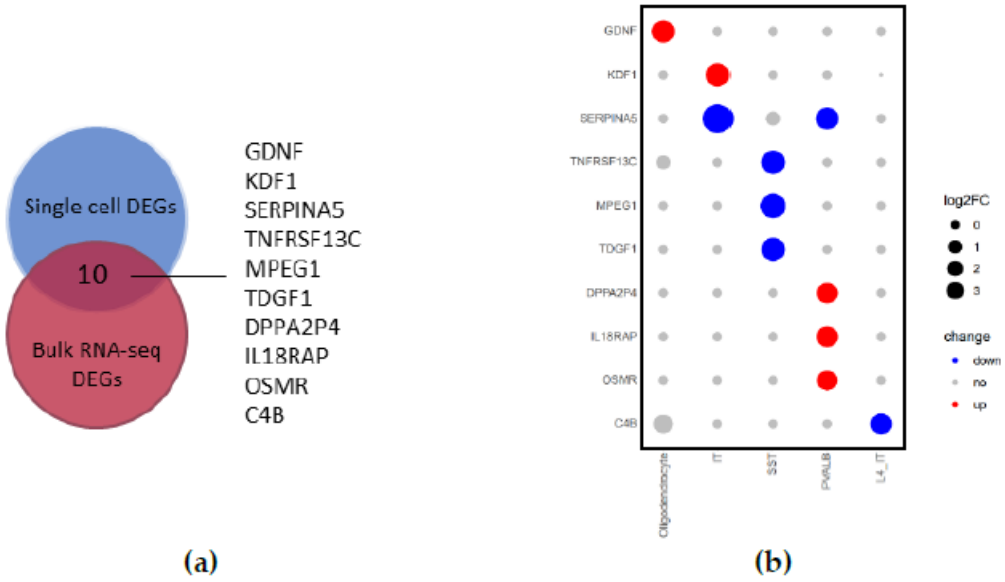

Figure 5. DEGs overlapped between bulk and sing cell RNA-seq. (**a**) Venn diagram of bulk and sing cell RNA-seq DEGs; (**b**) Dot plots showing the relative expression change of specific genes across different cell types. The size indicates the Log2FC values (SCZ/control), the color of red indicates upregulated, blue indicates downregulated, and grey indicates no change.

2.6. The relationships between each cell type identifying two major modules underlying SCZ

To explore the potential correlation between each cell type underlying SCZ, we plotted the Jaccard similarity heatmap of 17 cell types based on the similarity of the DEGs (figure 6). There were few DEGs of L5/6_IT_CAR3 cell types, so we omitted this cell type. We observed two correlative modules. One of the modules included three types of excitatory glutamatergic neurons (IT, L4_IT, L5/6_NP) and three types of inhibitory GABAergic neurons (LAMP5, SST, PAX6). The other module included four non-neuronal cell types (Astrocyte, Endothelial, Oligodendrocyte, Pericyte) and excitatory glutamatergic neuron (L6_CT). Overall, it suggested that some cell types might converge to a module to affect the SCZ.

Preprints (www.preprints.org) | NOT PEER-REVIEWED | Posted: 18 August 2022 doi:10.20944/preprints202208.0341.v1

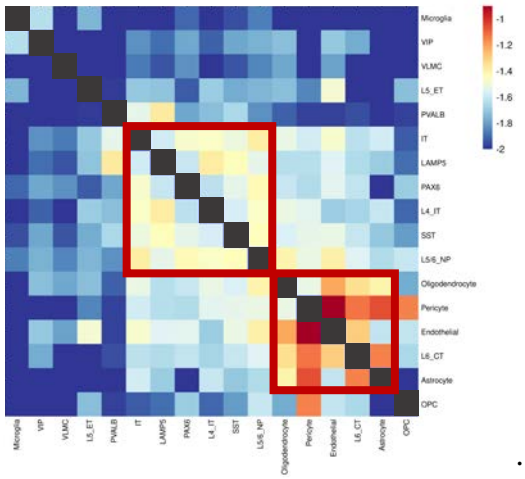

Figure 6. Heatmap showing neuronal and non-neuronal cell types grouped based on Jaccard similarity of the DEGs. Rows and columns correspond to cell types, and the intersection represents the Jaccard similarity between the two cell types. The red box indicates the cell types that converge to a module.

3. Discussion

Schizophrenia is a complex psychiatric disorder affected by various cell types in the brain. However, how individual cell types are affected by schizophrenia and how each cell type can contribute to schizophrenia occurrence is not completely clear. We sought to address the question by focusing on the integrative analyses of DLPFC bulk RNA-seq data and scRNA-seq data converted by the deconvolution algorithm CIBERSORTx. We could figure out how changes in the transcriptome of the schizophrenia DLPFC tissue were distributed across multiple cell types.

In this study, we presented the single-cell research of multiple cell types in the DLPFC of schizophrenia patients using CIBERSORTx and elucidated the cell type fraction changes and SCZ-related alterations in gene expression in each cell type at the single-cell level. First, after deconvolution of the bulk RNA-seq data with CIBERSORTx, the proportional distribution of 19 cell types in SCZ and normal tissues showed a different trend, astrocyte, pericyte, and PAX6 cells were found to have higher proportion in SCZ patients, while the L5/6_IT_CAR3 cells and LAMP5 cells are the exact opposite. Firstly, astrocyte can critically affect key neurodevelopmental and homeostatic processes pertaining to schizophrenia pathogenesis [32]. Our result is consistent with the previous study, which noted postmortem histological study identified that the number of astrocytes was increased in the brain of patients with schizophrenia [33], and the increased density of S100β $^{+}$ astrocytes was found in patients with paranoid schizophrenia [34]. Secondly, pericyte cell type, known as one of the neurovascular unit elements, brain imaging in SCZ patients reveals vascular dysfunction in PFC region using fMRI [35]. Lastly, GABAergic neurons, PAX6 and LAMP5, and Glutamatergic neurons, L5/6_IT_CAR3, which can establish inhibitory and excitatory synapses, the changes in their proportion may impact on alteration in GABAergic and glutamatergic balance [36].

Next, although bulk RNA-seq [37] have revealed some genes and pathways associated with SCZ, it could not resolve the cell type-specific pathology underlying SCZ. Using single-cell deconvolution analysis of the SCZ DLPFC region greatly increases the resolution of gene expression changes. Thus, we discovered that SCZ is characterized by the dysregulation of thousands of genes with up-/downregulation in specific cell types. In total, by summing up dysregulated genes across all cell types, ~4607 and 528 DEGs for

 doi:10.20944/preprints202208.0341.v1

neurons and non-neurons, respectively, and each cell type has cell-special DEGs. It suggested that the contribution of each cell type to SCZ occurrence differ in severity. On the one hand, in neurons, we reported that three GABAergic neurons: PVALB, LAMP5, SST cell types exhibited the largest transcriptomic effect in SCZ. GABAergic neurons play an essential role in regulating neurotransmission and maintaining a fine-tuned excitation-inhibition balance in the brain [38]. Firstly, we found that PVALB cell type exhibited abnormality in synaptic signaling and chemical synaptic transmission. The result is consistent with the glutamate hypothesis of schizophrenia states, which noted PVALB neurons mediated glutamate neurotransmission to attribute to the development of SCZ [39]. Secondly, LAMP5 neurons were among the cell types most affected by SCZ based on the changes in gene expression and cell-type proportion. LAMP5 interneurons exhibited abnormality in ATP metabolic process, NADH dehydrogenase complex assembly, chemical synaptic transmission, axo-dendritic transport, and axon development. This result suggested that LAMP5 neurons not only take part in GABAergic neurons common neurotransmission function, but also play an important role in energy metabolism in SCZ. Lastly, SST neurons exhibited abnormal in leukocyte cell-cell adhesion, leukocyte activation, T cell activation. In some mouse models, SST neurons have been shown to be associated with immune and neuroinflammation [40]. On the other hand, in non-neurons, we reported that oligodendrocytes exhibit the largest transcriptomic effect in SCZ. Here, oligodendrocytes exhibited abnormal in innate immune response and inflammatory response. Similarly, various studies also support that oligodendrocytes are directly involved in inflammation and immune modulation in CNS disease [41-42].

In addition, one of the major findings in our study is the discovery that the DEGs from bulk RNA-seq display different changes in the cellular level. For example, SERPINA5 gene exhibited a dramatic decrease in expression across two neuron cell types, IT and PVALB. SERPINA5 gene also exhibited downregulated in L5/6_NP and IT cell types, although they were not significant enough. Interestingly, SERPINA5 encodes a member of the serine protease inhibitor family of proteins, which has been implicated in synaptic plasticity and memory formation [43]. Angela M. Crist et al. reported that histologic and biochemical analyses suggested SERPINA5 expression dysregulation is associated with Alzheimer's disease [28]. SCZ and AD are two severe brain disorders that share considerable comorbidities in both clinical and genetic contexts [44]. Thus, the genetic influence of SERPINA5 on SCZ is also worth exploring.

Furthermore, considering that SCZ is caused by the cooperation of multiple cell types, we used Jaccard distance to identify two major cell type modules. The cell types converged to the same module exhibited similar coordinated transcriptomic changes. Firstly, three excitatory glutamatergic neurons (IT, L4_IT, L5/6_NP) and three inhibitory GABAergic neurons (LAMP5, SST, PAX6) clustered together according to changes in gene expression. This result suggested that two major neurons exist in coordinated shifts, inconsistent with the previous observation that glutamatergic and GABAergic neurons lost connection [45] in brain regions associated with SCZ. Secondly, the expression pattern of non-neuronal cell types was different from neuronal cell types. For example, the crosstalk between astrocytes and oligodendrocytes is important for glial development, triggering disease onset and progression, as well as stimulating regeneration and repair [46]. We also observed that glutamatergic neuron (L6_CT) exhibit similar expression change with non-neuronal cell types. It is reported that inflammatory cytokines such as IL-1β released from glia may facilitate signal transmission through its coupling to neuronal glutamate receptors [47]. This bidirectional neuron-glial signaling plays a key role in glial activation and cytokine production [48]. Overall, such modules of SCZ-related cell types can reveal the cooperation of multiple cell types, which may influence the occurrence of SCZ.

Taken together, although our current study has some limitations, we identify large-scale changes in the neuronal and non-neuronal transcriptomes of SCZ patients using CIBERSORTx, where some cell types displayed proportion changes and a dramatic SCZ-related cell-specific dysregulation of gene expression. Moreover, by integrating analyses

 doi:10.20944/preprints202208.0341.v1

of DLPFC bulk RNA-seq and scRNA-seq data, we reveal that the DEGs from bulk RNA-seq display different changes in cellular level. In addition, we discovered that different subtypes of neurons might exhibit coherent SCZ-related transcriptomic changes. Our result suggested SCZ therapies should take into consideration the genes and cell types heterogeneity. Thus, these findings strengthen our understanding of SCZ and can improve current therapeutic strategies for this disorder.

4. Materials and Methods

4.1. Data Collection

We obtained the single-cell transcriptome data of 6,468 cells with normal adult middle temporal gyrus (MTG) and anterior cingulate cortex (ACC) from ALLEN BRAIN MAP [16], [17] (https://portal.brain-map.org/atlases-and-data/rnaseq/human-multiple-cortical-areas-smart-seq). The human dorsolateral prefrontal cortex (DLPFC) RNA-seq data in this study were collected from BrainSeq Phase 2[18] (http://eqtl.brainseq.org/phase2), consisting of 138 SCZ cases and 251 control samples over 18 years of age.

4.2. Impute Cell Fractions with CIBERSORTx

To characterize the abundance of 19 cell types based on the RNA-seq data in DLPFC tissues, we applied CIBERSORTx web tool, a machine learning method that infers cell-type-specific gene expression profiles without physical cell isolation. We first prepared and uploaded the single-cell expression matrix according to the instructions with CIBERSORTx. All parameters used the default values suggested by the tool developers. Then we ran "CIBERSORTx" and obtained a signature matrix of 19 cell types from scRNA-seq data.

Next, we loaded the datasets of SCZ patients and healthy subjects samples into CIBERSORTx according to the instructions. After inputting the cell type signature matrix, we acquired the relative proportions of 19 neuronal and non-neuronal cells in each sample with a p-value corresponding to the confidence of the results for the deconvolution. Because the scRNA-seq data was derived from Smart-seq2 platform [19], we selected "B-mode" for batch correction and 1,000 permutation tests. Other parameters used the default values.

4.3. Bulk RNA-seq differentially Expressed Gene Analysis

We analyzed the bulk RNA-Seq data of 138 SCZ cases and 251 control samples obtained from BrainSeq Phase 2. The analysis was performed using package "DESeq-2 [20]", "limma[21]", "edgeR[22]" . Setting the cut-off criteria as $|\log2 \text{ fold change}| > 0.5$ and FDR < 0.05, we identified 108 differentially expressed genes (DEGs) that reached the significance threshold in all three methods.

4.4. Impute Cell-Type-Specific Gene Expression with CIBERSORTx

To impute cell type-specific gene expression, we performed CIBERSORTx group-mode on SCZ and normal classes from BrainSeq Phase 2 separately. Using filtered gene expression profiles, we identified statistically significant differentially expressed genes of each cell type using the R script provided by the guideline. The cut-off criteria were false discovery rate (FDR) of <0.05 and $|\log2 \text{ fold change}| > 1.5$.

4.5. Gene ontology (GO) analysis

We performed a GO enrichment analysis of the DEGs of each cell type by Metascape [23]. Functional enrichment was performed in three GO categories: biological process, molecular function, and cellular component. Terms with $p < 0.05$, a minimum count of 3, and an enrichment factor of >1.5 (the enrichment factor was defined as the observed count's ratio to the count expected by chance) were collected and grouped into clusters based on

their membership similarities. Furthermore, p-values were calculated based on the cumulative hypergeometric distribution. The p-values of the hypergeometric tests were adjusted for multiple testing by the Benjamin–Hochberg method.

4.6. Jaccard similarity between each cell types

To explore the relationships between each cell type underlying the SCZ, we estimated the Jaccard similarity on the DEGs of each cell type.

$$\text{Jaccard similarity} = \frac{N_{\text{both cell types}}}{N_{\text{either cell type}}}$$

For the visualization, we clustered Jaccard similarity using hierarchical clustering (R functions hclust with parameter method = "ward.D").

Supplementary Materials: The following supporting information can be downloaded at: www.mdpi.com/xxx/s1, Table S1: All DEGs for each neuronal cell type in this study; Table S2: All DEGs for each non-neuronal cell type in this study.

Author Contributions: Conceptualization, W.C., W.S. and G.N.L.; methodology, W.C. and W.S.; software, Z.L. and D.T.M.; validation, W.S. and G.N.L.; formal analysis, J.L.; investigation, W.C. and W.S.; resources, J.L.; data curation, W.C.; writing—original draft preparation, W.C.; writing—review and editing, W.C., W.S. and G.N.L.; visualization, W.C., Z.L. and D.T.M.; supervision, G.N.L.; project administration, G.N.L.; funding acquisition, G.N.L. All authors have read and agreed to the published version of the manuscript.

Funding: This work was supported by grants from the National Natural Science Foundation of China (nos. 81971292, 82150610506), Natural Science Foundation of Shanghai (No: 21ZR1428600).

Institutional Review Board Statement: Not applicable

Informed Consent Statement: Not applicable

Data Availability Statement: All data analyzed in this study are curated from the public domain.

Conflicts of Interest: The authors declare no conflict of interest.

References

1. G. Kuperberg and S. Heckers, "Schizophrenia and cognitive function," Current Opinion in Neurobiology, vol. 10, no. 2, pp. 205–210, Apr. 2000, doi: 10.1016/S0959-4388(00)00068-4.
2. T. Zhang et al., "Voltage-gated calcium channel activity and complex related genes and schizophrenia: A systematic investigation based on Han Chinese population," Journal of Psychiatric Research, vol. 106, pp. 99–105, Nov. 2018, doi: 10.1016/J.JPSYCHIRES.2018.09.020.
3. J. L. Rapoport, A. M. Addington, S. Frangou, and M. R. C. Psych, "The neurodevelopmental model of schizophrenia: update 2005," Molecular Psychiatry 2005 10:5, vol. 10, no. 5, pp. 434–449, Feb. 2005, doi: 10.1038/sj.mp.4001642.
4. S. G. Potkin et al., "Working memory and DLPFC inefficiency in schizophrenia: The FBIRN study," Schizophrenia Bulletin, vol. 35, no. 1, pp. 19–31, Jan. 2009, doi: 10.1093/SCHBUL/SBN162.
5. E. S. Finn, L. Huber, D. C. Jangraw, P. J. Molfese, and P. A. Bandettini, "Layer-dependent activity in human prefrontal cortex during working memory," Nature Neuroscience 2019 22:10, vol. 22, no. 10, pp. 1687–1695, Sep. 2019, doi: 10.1038/s41593-019-0487-z.
6. C. R. Sullivan, R. H. Koene, K. Hasselfeld, S. M. O'Donovan, A. Ramsey, and R. E. McCullumsmith, "Neuron-specific deficits of bioenergetic processes in the dorsolateral prefrontal cortex in schizophrenia," Molecular Psychiatry, vol. 24, no. 9, pp. 1319–1328, Sep. 2019, doi: 10.1038/s41380-018-0035-3.
7. J. Smucny, S. J. Dienel, D. A. Lewis, and C. S. Carter, "Mechanisms underlying dorsolateral prefrontal cortex contributions to cognitive dysfunction in schizophrenia," Neuropsychopharmacology 2021 47:1, vol. 47, no. 1, pp. 292–308, Jul. 2021, doi: 10.1038/s41386-021-01089-0.
8. D. C. Koboldt et al., "A de novo nonsense mutation in ASXL3 shared by siblings with Bainbridge-Ropers syndrome.," Cold Spring Harb Mol Case Stud, vol. 4, no. 3, p. a002410, Jun. 2018, doi: 10.1101/mcs.a002410.
9. D. L. Braff et al., "The Generalized Pattern of Neuropsychological Deficits in Outpatients With Chronic Schizophrenia With Heterogeneous Wisconsin Card Sorting Test Results," Archives of General Psychiatry, vol. 48, no. 10, pp. 891–898, Oct. 1991, doi: 10.1001/ARCHPSYC.1991.01810340023003.

10. D. H. R. Blackwood, D. M. Clair, W. J. Muir, and J. C. Duffy, "Auditory P300 and Eye Tracking Dysfunction in Schizophrenic Pedigrees," Archives of General Psychiatry, vol. 48, no. 10, pp. 899–909, Oct. 1991, doi: 10.1001/ARCHPSYC.1991.01810340031004.
11. R. Kim, K. L. Healey, M. T. Sepulveda-Orengo, and K. J. Reissner, "Astroglial correlates of neuropsychiatric disease: From astrocytopathy to astrogliosis," Progress in Neuro-Psychopharmacology and Biological Psychiatry, vol. 87, pp. 126–146, Dec. 2018, doi: 10.1016/J.PNPBP.2017.10.002.
12. L. Samartzis, D. Dima, P. Fusar-Poli, and M. Kyriakopoulos, "White Matter Alterations in Early Stages of Schizophrenia: A Systematic Review of Diffusion Tensor Imaging Studies," Journal of Neuroimaging, vol. 24, no. 2, pp. 101–110, Mar. 2014, doi: 10.1111/J.1552-6569.2012.00779.X.
13. N. G. Skene et al., "Genetic identification of brain cell types underlying schizophrenia," Nature Genetics, vol. 50, no. 6, pp. 825–833, Jun. 2018, doi: 10.1038/s41588-018-0129-5.
14. M. Lam et al., "Comparative genetic architectures of schizophrenia in East Asian and European populations," Nature Genetics 2019 51:12, vol. 51, no. 12, pp. 1670–1678, Nov. 2019, doi: 10.1038/s41588-019-0512-x.
15. A. M. Newman et al., "Determining cell type abundance and expression from bulk tissues with digital cytometry," Nature Biotechnology 2019 37:7, vol. 37, no. 7, pp. 773–782, May 2019, doi: 10.1038/s41587-019-0114-2.
16. B. Tasic et al., "Shared and distinct transcriptomic cell types across neocortical areas," Nature 2018 563:7729, vol. 563, no. 7729, pp. 72–78, Oct. 2018, doi: 10.1038/s41586-018-0654-5.
17. R. D. Hodge et al., "Conserved cell types with divergent features in human versus mouse cortex," Nature 2019 573:7772, vol. 573, no. 7772, pp. 61–68, Aug. 2019, doi: 10.1038/s41586-019-1506-7.
18. L. Collado-Torres et al., "Regional Heterogeneity in Gene Expression, Regulation, and Coherence in the Frontal Cortex and Hippocampus across Development and Schizophrenia," Neuron, vol. 103, no. 2, pp. 203-216.e8, Jul. 2019, doi: 10.1016/J.NEURON.2019.05.013.
19. S. Picelli, O. R. Faridani, Å. K. Björklund, G. Winberg, S. Sagasser, and R. Sandberg, "Full-length RNA-seq from single cells using Smart-seq2," Nature Protocols 2013 9:1, vol. 9, no. 1, pp. 171–181, Jan. 2014, doi: 10.1038/nprot.2014.006.
20. M. I. Love, W. Huber, and S. Anders, "Moderated estimation of fold change and dispersion for RNA-seq data with DESeq2," Genome Biology, vol. 15, no. 12, pp. 1–21, Dec. 2014, doi: 10.1186/S13059-014-0550-8/FIGURES/9.
21. G. K. Smyth, "limma: Linear Models for Microarray Data," Bioinformatics and Computational Biology Solutions Using R and Bioconductor, pp. 397–420, Dec. 2005, doi: 10.1007/0-387-29362-0_23.
22. M. D. Robinson, D. J. McCarthy, and G. K. Smyth, "edgeR: a Bioconductor package for differential expression analysis of digital gene expression data," Bioinformatics, vol. 26, no. 1, pp. 139–140, Jan. 2010, doi: 10.1093/BIOINFORMATICS/BTP616.
23. Y. Zhou et al., "Metascape provides a biologist-oriented resource for the analysis of systems-level datasets," Nature Communications, vol. 10, no. 1, pp. 1–10, Dec. 2019, doi: 10.1038/s41467-019-09234-6.
24. C. B. Steen, C. L. Liu, A. A. Alizadeh, and A. M. Newman, "Profiling cell type abundance and expression in bulk tissues with CIBERSORTx," Methods in Molecular Biology, vol. 2117, pp. 135–157, 2020, doi: 10.1007/978-1-0716-0301-7_7/FIGURES/4.
25. C. Bayly-Jones, S. S. Pang, B. A. Spicer, J. C. Whisstock, and M. A. Dunstone, "Ancient but Not Forgotten: New Insights Into MPEG1, a Macrophage Perforin-Like Immune Effector," Frontiers in Immunology, vol. 11, p. 2690, Oct. 2020, doi: 10.3389/FIMMU.2020.581906/BIBTEX.
26. Q. Wu, W. Kong, and S. Wang, "Peripheral Blood Biomarkers CXCL12 and TNFRSF13C Associate with Cerebrospinal Fluid Biomarkers and Infiltrating Immune Cells in Alzheimer Disease," Journal of Molecular Neuroscience, vol. 71, no. 7, pp. 1485–1494, Jul. 2021, doi: 10.1007/S12031-021-01809-7/FIGURES/4.
27. J. M. De La Cruz et al., "A loss-of-function mutation in the CFC domain of TDGF1 is associated with human forebrain defects," Human Genetics 2002 110:5, vol. 110, no. 5, pp. 422–428, Apr. 2002, doi: 10.1007/S00439-002-0709-3.
28. A. M. Crist et al., "Transcriptomic analysis to identify genes associated with selective hippocampal vulnerability in Alzheimer's disease," Nature Communications 2021 12:1, vol. 12, no. 1, pp. 1–17, Apr. 2021, doi: 10.1038/s41467-021-22399-3.
29. H. Liu et al., "Identification of IL18RAP/IL18R1 and IL12B as Leprosy Risk Genes Demonstrates Shared Pathogenesis between Inflammation and Infectious Diseases," The American Journal of Human Genetics, vol. 91, no. 5, pp. 935–941, Nov. 2012, doi: 10.1016/J.AJHG.2012.09.010.
30. Z. Tunca et al., "Diverse Glial Cell Line-Derived Neurotrophic Factor (GDNF) Support Between Mania and Schizophrenia: A Comparative Study in Four Major Psychiatric Disorders," European Psychiatry, vol. 30, no. 2, pp. 198–204, Feb. 2015, doi: 10.1016/J.EURPSY.2014.11.003.
31. P. Griffin et al., "Rev-erbα mediates complement expression and diurnal regulation of microglial synaptic phagocytosis," Elife, vol. 9, pp. 1–17, Dec. 2020, doi: 10.7554/ELIFE.58765.
32. T. Notter, "Astrocytes in schizophrenia.," Brain Neurosci Adv, vol. 5, p. 23982128211009148, Apr. 2021, doi: 10.1177/23982128211009148.
33. T. P. Schnieder and A. J. Dwork, "Searching for Neuropathology: Gliosis in Schizophrenia," Biological Psychiatry, vol. 69, no. 2, pp. 134–139, Jan. 2011, doi: 10.1016/J.BIOPSYCH.2010.08.027.
34. J. Steiner et al., "S100B-immunopositive glia is elevated in paranoid as compared to residual schizophrenia: A morphometric study," Journal of Psychiatric Research, vol. 42, no. 10, pp. 868–876, Aug. 2008, doi: 10.1016/J.JPSYCHIRES.2007.10.001.

35. M. Carrier, J. Guilbert, J. P. Lévesque, M. È. Tremblay, and M. Desjardins, "Structural and Functional Features of Developing Brain Capillaries, and Their Alteration in Schizophrenia," Frontiers in Cellular Neuroscience, vol. 14, p. 456, Jan. 2021, doi: 10.3389/FNCEL.2020.595002/BIBTEX.
36. G. M. Quiñones, A. Mayeli, V. E. Yushmanov, H. P. Hetherington, and F. Ferrarelli, "Reduced GABA/glutamate in the thalamus of individuals at clinical high risk for psychosis," Neuropsychopharmacology 2020 46:6, vol. 46, no. 6, pp. 1133–1139, Dec. 2020, doi: 10.1038/s41386-020-00920-4.
37. C. A. Benson et al., "Immune Factor, TNFα, Disrupts Human Brain Organoid Development Similar to Schizophrenia—Schizophrenia Increases Developmental Vulnerability to TNFα," Frontiers in Cellular Neuroscience, vol. 14, p. 233, Aug. 2020, doi: 10.3389/FNCEL.2020.00233/BIBTEX.
38. L. Nahar, B. M. Delacroix, and H. W. Nam, "The Role of Parvalbumin Interneurons in Neurotransmitter Balance and Neurological Disease," Frontiers in Psychiatry, vol. 12, p. 679960, Jun. 2021, doi: 10.3389/FPSYT.2021.679960.
39. O. Marín, "Interneuron dysfunction in psychiatric disorders," Nat Rev Neurosci, vol. 13, no. 2, pp. 107–120, Feb. 2012, doi: 10.1038/NRN3155.
40. R. J. Duchatel et al., "Reduced cortical somatostatin gene expression in a rat model of maternal immune activation," Psychiatry Research, vol. 282, p. 112621, Dec. 2019, doi: 10.1016/J.PSYCHRES.2019.112621.
41. E. P. Harrington, D. E. Bergles, and P. A. Calabresi, "Immune cell modulation of oligodendrocyte lineage cells," Neuroscience Letters, vol. 715, p. 134601, Jan. 2020, doi: 10.1016/J.NEULET.2019.134601.
42. P. M. Madsen et al., "Oligodendrocytes modulate the immune-inflammatory response in EAE via TNFR2 signaling," Brain, Behavior, and Immunity, vol. 84, pp. 132–146, Feb. 2020, doi: 10.1016/J.BBI.2019.11.017.
43. A. G. Almonte and J. D. Sweatt, "Serine proteases, serine protease inhibitors, and protease-activated receptors: Roles in synaptic function and behavior," Brain Research, vol. 1407, pp. 107–122, Aug. 2011, doi: 10.1016/J.BRAINRES.2011.06.042.
44. M. A. A. Demichele-Sweet et al., "Genetic risk for schizophrenia and psychosis in Alzheimer disease," Molecular Psychiatry 2018 23:4, vol. 23, no. 4, pp. 963–972, May 2017, doi: 10.1038/mp.2017.81.
45. D. K. Shukla et al., "Anterior Cingulate Glutamate and GABA Associations on Functional Connectivity in Schizophrenia," Schizophrenia Bulletin, vol. 45, no. 3, pp. 647–658, Apr. 2019, doi: 10.1093/SCHBUL/SBY075.
46. E. Nutma, D. van Gent, S. Amor, and L. A. N. Peferoen, "Astrocyte and Oligodendrocyte Cross-Talk in the Central Nervous System," Cells 2020, Vol. 9, Page 600, vol. 9, no. 3, p. 600, Mar. 2020, doi: 10.3390/CELLS9030600.
47. S. Yang, Z. W. Liu, L. Wen, H. F. Qiao, W. X. Zhou, and Y. X. Zhang, "Interleukin-1beta enhances NMDA receptor-mediated current but inhibits excitatory synaptic transmission," Brain Res, vol. 1034, no. 1–2, pp. 172–179, Feb. 2005, doi: 10.1016/J.BRAINRES.2004.11.018.
48. K. Ren and R. Dubner, "Neuron-glia crosstalk gets serious: Role in pain hypersensitivity," Curr Opin Anaesthesiol, vol. 21, no. 5, p. 570, Oct. 2008, doi: 10.1097/ACO.0B013E32830EDBDF.